ETH
Eidgenössische Technische Hochschule Zürich
Swiss Federal Institute of Technology Zurich

Ion response to endcap voltage variations in a linear Paul trap

Semester Thesis

Frederike Brockmeyer

Monday 25th July, 2022
v3.1

Advisors: Dr. N. S. Hedrich,
Prof. Dr. J. Home

Department of Physics, ETH Zürich

Abstract

We analysed the response of Barium ions in a Paul trap to the variation of the voltages on the endcap electrodes. The goal was to aid with the characterization of the electric field in a linear Paul trap located at the Swiss Science Center Technorama, and to find a voltage range in which ions can be stably trapped. We also attempted to determine the numerical value of the elementary charge, e, using data from this trap, as this could be a task given to student classes visiting the Swiss Science Center Technorama. The characterization of the trap unveiled asymmetries in the setup.

Contents

Chapter 1

Background

1.1 Introduction

An ion trap is an apparatus that uses electric or magnetic fields to fix ions in a nearly stationary, controllable position. Since the first mention of the word 'trapping' in the book 'Theory and Design of Electron Beams' (1949) by J.R. Pierce [1], [2], physicists have designed traps able to confine, individually control and fully entangle multiple ions [3]. Trapped ions are one of the leading architectures currently developed for quantum computing, but up until very recently, the experience of seeing and experimenting with single ions was one limited to the lab. In co-operation with the Swiss Science Center Technorama (SSCT), the Trapped Ion Quantum Information group at ETH Zurich designed an exhibit of a Barium ion trap, which is now displayed at the SSCT.

The SSCT aims to be 'a place designed for self-directed discovery, comprehension and understanding' [4], and as such it is 'the largest out-of-school learning institution for the sciences in Switzerland' [4]. The goal of this exhibit is to allow visitors of all ages to independently discover some properties of ions, such as the concept of a lifetime of an exited state, and the role of the ions charge in the trapping mechanism. The exhibit should also improve the public's understanding of some of the current research in the field of quantum information science.

In this project, we worked towards improving the visitors experience of the setup by developing workshops for classes that would improve their understanding of the exhibit. In the first chapter we describe the setup at the SSCT. We then analyse the position of the ions when varying the endcap voltages of the setup in the second chapter. This information is used to design a student workshop at SSCT, as described in chapter three.

1.2 Theory

In order to make ions visible to the observer, we must fist ionize them. Then we must cool them and apply an electric field so that they are trapped. Finally we must stimulate them into exited energy states so that they can emit visible light. The trapping, cooling and excitation process will be described in this section

1.2.1 Trapping potential of a Paul trap

As stated by Earnshaw, it is impossible to confine a charged particle in a space using only electrostatic fields [5]. A Paul trap therefore uses a combination of electrostatic and radio frequency fields to create an effective three dimensional harmonic pseudopotential at the center of the trap. Along the symmetry axis[1], this harmonic potential can be characterized by a trap frequency ν, which is found through numerical simulations of the electric potential in a trap geometry. If more than one ion is loaded into the trap, the ions will also experience the Coulomb repulsion of the other ions. The full potential energy experienced by N ions placed along the symmetry axis of the trap, z, will therefore be:

$$V = \sum_{m=1}^{N} \frac{1}{2} M\nu^2 z_m(t)^2 + \sum_{\substack{n,m=1 \\ m\neq n}}^{N} \frac{Z^2 e^2}{8\pi\varepsilon_0} \frac{1}{|z_n(t) - z_m(t)|} \quad [6], \tag{1.1}$$

where M is the mass of an ion, z_m is the position of the m-th ion, Z is the charge number of the ions, e is the elementary charge and ε_0 is the permittivity of free space. The first term describes the potential energy of a charge in a harmonic potential, while the second describes the potential energy due to the interaction of the charges, the Coulomb potential. The minimum of the harmonic potential lies in the center of the trap, at $z = 0$, so if the ions have sufficiently low kinetic energy, they will be trapped in this position. The cooling mechanism is discussed later.

1.2.2 Ion configurations in a Paul trap

Eq. 1.1 shows that an increase in the trap frequency ν will lead to a steeper harmonic potential along the symmetry axis, and hence decrease in the spacing between ions in equilibrium. This spacing can be determined numerically using the ansatz $\frac{\partial V}{\partial z_m} = 0$, and solving the resulting system of simultaneous equations. The equilibrium positions are used to find the smallest distance Δz between the N trapped ions [6]. In the case of two and three ions, the distance was calculated analytically, as shown in Appendix A. In the general

[1] The *symmetry axis* is the axis on which the ions chain is trapped.

case, i.e. $N = n$, this is not possible, and the system of equations is solved numerically. One can then find an approximate relationship between the number of ions and the N and the smallest distance Δz,

$$\begin{aligned} N = 2 : \Delta z &= 2\, l\, \left(\frac{1}{2}\right)^{2/3} \\ N = 3 : \Delta z &= l\, \left(\frac{5}{4}\right)^{1/3} \\ N = n, n \in \mathbb{N} : \Delta z &\approx l\, \frac{2.018}{n^{0.559}}, \end{aligned} \tag{1.2}$$

where $l^3 = \frac{Z^2 e^2}{4\pi\varepsilon_0 M \nu^2}$. Other approximations can also be made, for example $\Delta z_{\min} \approx l\, \frac{2.29}{n^{-0.596}}$ [7], or $\Delta z_{\min} \approx l\, \frac{2.0}{n^{-0.57}}$ [8]. A choice of approximation would become relevant, if one measured Δx for ion numbers larger than three ions.

At this point it should be noted that Eq. 1.1 and the respective definition of the trap frequency ν assume that the trap experiences a perfectly symmetric potential provided by the electrodes in the Paul trap. The data analysis will show that this is not a realistic assumption. It should also be noted that the derivation assumes a one dimensional potential, so ions are fully restricted to movement on the symmetry axis. This may not be the case for large trap frequencies, in which case ions may position themselves in a zig-zag configuration around the symmetry axis instead.

1.2.3 Doppler cooling

The ions are made visible through the Doppler cooling mechanism, which uses lasers waves detuned to lower the average kinetic energy of a trapped ion [9]. This can be illustrated by analyzing the energy level spectrum of a suitable ion, such as ^{138}Ba+, shown in Fig. 1.1. Here, the relevant resonance wavelength used for Doppler cooling is between 493 nm and 494 nm, as a the high transition rate of 14.66 MHz causes a fast re-emission of the absorbed photon, and hence allows for an efficient cooling process. If the laser is tuned from this resonance, the relativistic Doppler effect ([10]) will only allow counterpropagating ions to absorb the laser's photons, and experience the corresponding impulse opposing their motion. Since the photon is then re-emitted in a random direction, the ion will likely lose overall kinetic energy. If the light reaches the ions from many different directions, and the ions will be cooled. It is important to note that this wavelength lies within the visible range, so the light emitted by the ions through the cooling process can simultaneously be used to observe the ions with the human eye. Since the 493 nm laser can only drive the transition from the $6\,^2S_{1/2}$ state to the $6\,^2P_{1/2}$ state, the ions must not leave these two states to remain visible. Hence we

will call state $6\,^2S_{1/2}$ the *bright* state. All states that cannot be driven with the 493 nm laser will be called *dark* states[2].

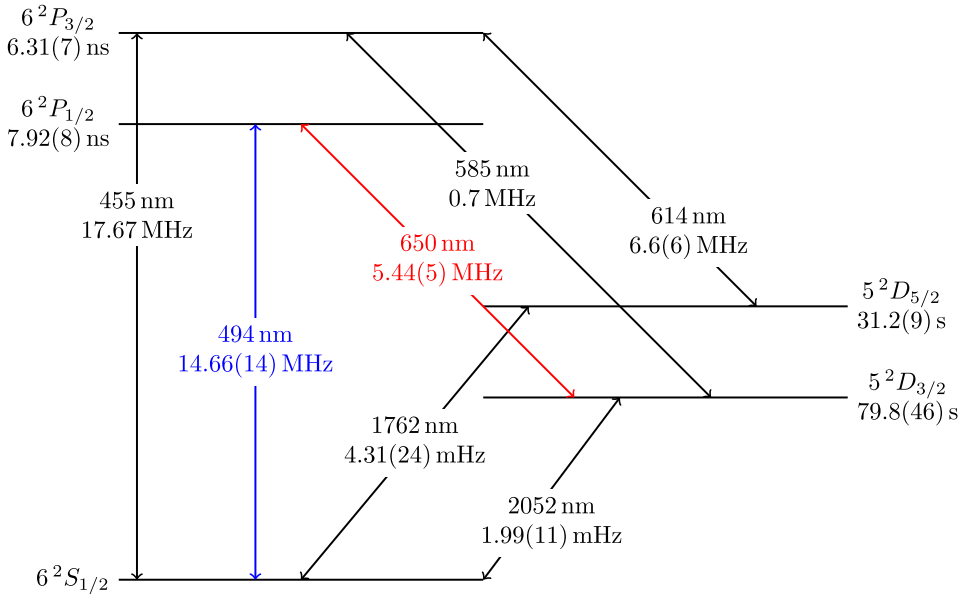

Figure 1.1: This diagram shows the five lowest states of the energy level spectrum of a Ba^+_{56} ion at zero magnetic field. Each state is labelled with the corresponding Russel-Saunders term symbol, $n^{2S+1}L_J$, where n is the principal quantum number, S is the total spin, L is the total orbital angular momentum and J is the total angular momentum. For each possible transition, the diagram shows the wavelength of the emitted photon and the transition frequency. This Figure is taken from [11].

1.3 The barium trap at Technorama

In this project, we varied the positions of the ions within the barium Paul trap at SSCT (Fig. 1.2), and then observed the effect on their configuration from the outside. The ions could be moved by varying the voltages of the electrodes within the setup, which are individually adjustable. The ions could then be observed through a lens with 20 times magnification from one side (label '1' in Fig. 1.2a), and a continuous video stream transmitted to a server using a camera on the other side (label '2' in Fig. 1.2a).

[2]It is possible to make an ion intentionally invisible by driving the 455 nm transition from $6\,^2S_{1/2}$ to $6\,^2P_{3/2}$, from where the ion will quickly decay into the $5\,^2D_{5/2}$ state, which has a slow decay rate of 4.31 mHz. In order to avoid an unintentional decay from $6^2P_{1/2}$ into another *dark* state, $5^2D_{3/2}$, the 650 nm transition has to be driven continuously, which is also done on the setup.

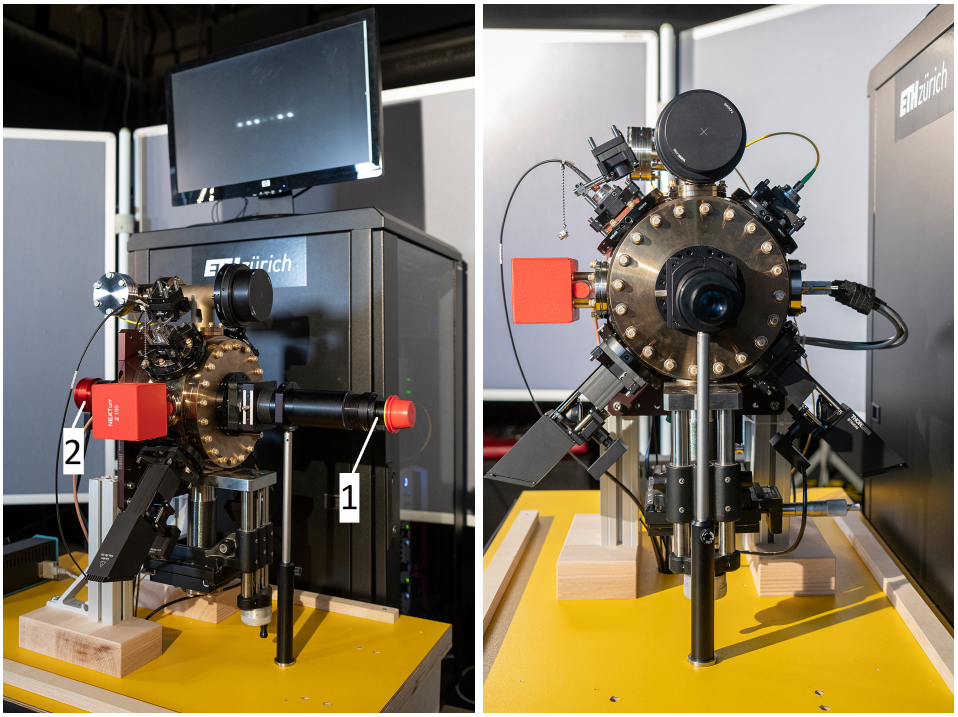

(a) (b)

Figure 1.2: Setup at SSCT. Image (a) shows a side view of the setup, while (b) shows the view from the perspective of the visitor looking at the eyepiece. The label '1' points to the eyepiece, while the label '2' points to the camera.

1.3.1 Arrangement of the electrodes

The Paul trap employs four radio frequency electrodes, two of which are operating at 2.8 MHz with an amplitude of about 400 V, and two of which are grounded, which produces an effective harmonic pseudopotential that traps the ions along the radial axes[3]. Two endcap electrodes at either end of the symmetry axis are used in combination with the ground electrodes to produce the harmonic potential along the symmetry axis, which was discussed in Sec. 1.2.1. The two endcap electrodes can each be tuned from -10 V to 10 V independently of each other. Note that we would need to apply equal positive potentials to produce a symmetric potential such as in Eq. 1.1. Furthermore, there are four wires, to which we can apply voltages between -10 V and 10 V for fine tuning of the ion positions along the radial axes. The setup is shown in Fig. 1.3. The camera is on the positive side of the x axis, hence 1a is the right endcap and 1b is the left endcap. The *center* of the trap is the point of relection, which is located on the symmetry axis halfway

[3]The *radial axes* are the axes orthogonal to the symmetry axis, which will be labelled x and y.

between the two endcaps. It is also the point onto which the light used for Doppler cooling is focused.

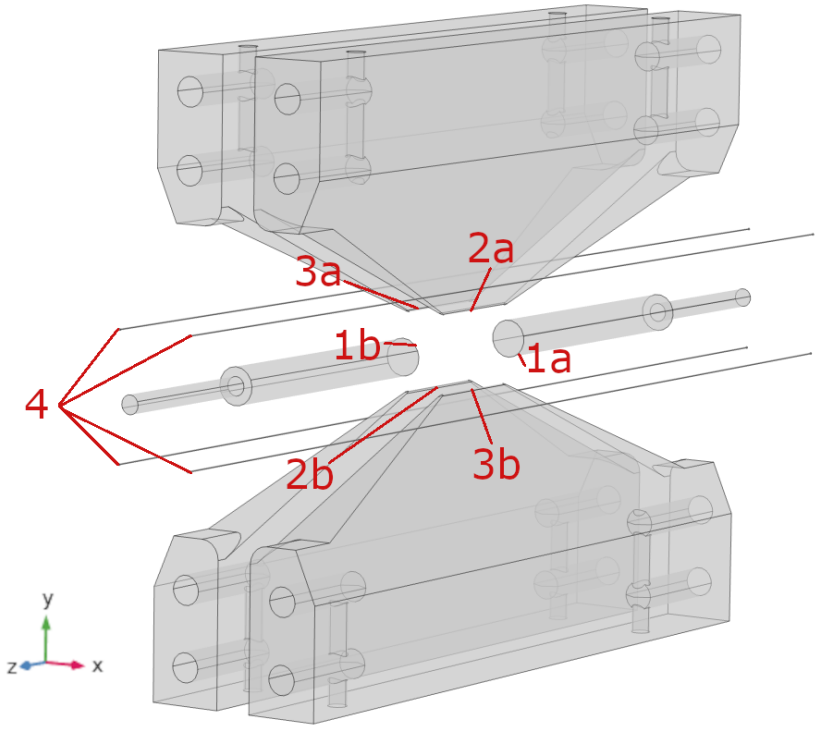

Figure 1.3: Diagram of the electrodes in the Paul trap at Technorama. *1 (a,b)* are the endcap electrodes, *2 (a,b)* are the radio frequency electrodes, *3 (a,b)* are the ground electrodes and *4* are the wires for fine tuning. The symmetry axis is labelled z, while the radial axes are labelled x and y. The ions are viewed along the x axis. The COMSOL Multiphysics® geometry was implemented by Ilia Sergachev.

1.3.2 Image properties

In this project, we chose to observe the ions using the video stream of the camera, as this would allow us to save pictures of their configuration, and hence analyse their positions quantitatively. The distance between the centers of the ions could be measured by converting the pixel size into physical units. There is a two lens system with focal lengths $f_1 = 100$ mm and $f_2 = 9.43$ mm set up in front of the camera to achieve a magnification of $\frac{f_1}{f_2} = 10.6$ [12]. The pixel size of the camera sensor, Sony IMX290LQR, is $L_{\text{pixel}} = 2.9$ µm [13]. The true distance Δz between two ions is therefore

$$\Delta z = \frac{L_{\text{pixel}}\, f_2}{f_1}\, n_{\text{pixel}} \approx 0.273\, n_{\text{pixel}}\ \mu\text{m}, \tag{1.3}$$

where n_{pixel} is the number of pixels between the centers of the two ions.

Chapter 2

Analysis of ion positions

In this chapter we quantify the response of ions to variations in the endcap voltages. Specifically, the range of endcap voltages, for which the ions were distinctly visible, is found. This information simplifies maintanance of the trap. It can also be used to make the exhibit more interactive, as we could now allow visitors to change the voltages of the endcap electrodes, which would move the ions along the symmetry axis. This could help the visitors gain an intuition for the relationship between charges and electric fields, and it will lay the foundation for more involved projects that can be given to visiting student classes at a later stage. Through the characterization of the trap potential, an asymmetry was identified, which is also analysed.

2.1 Measurement technique

In order to carry out these measurements, we need to be able to adjust the endcap voltages to different values, save images from the video stream after the voltages have been set, and read out the position of the ions from the image. Since the two endcap voltages can be adjusted independently, we are working in a two dimensional parameter space. It is therefore necessary to test thousands of combinations of the voltages, so the data analysis has been largely automatized using a Python script.

The majority of the image analysis was previously implemented by Albert Mitjans-Coma, who wrote a script [14], which, among other things, supplies a Remote Dictionary Server (Redis) with the current image of the video stream, as well as the pixel coordinates of the ions in the trap, and their corresponding brightness. The coordinates are found by applying the difference of Gaussians feature enhancement algorithm, and then searching for the pixel with maximum brightness in the vicinity of each ion. This image analysis script continuously runs on the local server of the setup.

Our script was also run on the local server of the setup, as it could then communicate with the digital to analogue converter (DAC) connected to the electrodes, and it could retrieve all relevant data from Redis. For each data point, the script would set the electrodes to the corresponding voltages, wait three seconds, and then request the image data from Redis. The idle time was needed to wait for the electrodes to respond and the image analysis code to update Redis.

Sometimes, one or more ions would no longer be detectable after changing the endcap voltages. This could be because the ions had been shifted out of the frame of the image, or they had been shifted so far from the center of the trap that they were no longer in focus of the 493 nm laser. If this had been the case, the corresponding endcap voltages should correctly have been labelled 'out of bounds' and should no longer be applied. However, often it was the case that the ions were not detected due to a temporary effect, such as an unstable laser (e.g. unlocked frequencies), a delayed response of the endcap electrodes, or noise causing an unintentional excitation into a dark state discussed in sec 1.2.3. In this case, a set of voltages could have been falsely labelled as 'out of bounds', or an ion could have been misidentified as the dark ion, and hence cause an error in the measured coordinate. To avoid this, the waiting time could be extended by the script if a change in ion number was detected.

The loading and unloading of ions had to be done manually, so the script was run separately for different numbers of ions in the trap. It would stop if an ion was lost during the scan and could not be recovered.

2.2 Determination of boundary voltages

An *asymmetry* in the endcap voltages occurs when the voltage of one endcap is different from the other. This can be done intentionally to move the ion along the symmetry axis, but it can also occur when the voltage supplied by the DAC is different from the voltage arriving at the endcap, resulting in a systematic error. This could for example be due coupling between the radio frequency line and the static line connected to one of the endcaps. Such a systematic error could then be dependent on the voltage in the static line, and would have to be analysed in detail, which is done in Sec. 2.3.

When varying the endcap voltages, it is possible to lose ions from the trap if this asymmetry between the endcap voltages is too large. It is also possible that the ions are simply off frame, or so close together that they are not distinguishable (Figure 2.1). Alternatively, the image of the ions may lose quality when the ions are not centered and therefore not properly illuminated by the lasers (Figure 2.2). It is therefore important to quantify these effects,

and determine which voltages provide us with a clear image[1] of the ions.

The clarity of an image was classified on a scale of zero to three. 'Zero' would mean that some ions were out of frame, no ions were visible or all ions were indistinguishable. 'One' would mean that the ions were very dim, such as in Fig. 2.2c, and hence not clearly visible, or most ions were indistinguishable to to the formation of a cloud, such as in Fig. 2.1d. 'Two' would mean that ions are visible but dim, such as in Fig. 2.2b, or the two/three middle ions were hard to distinguish as they were too close. 'Three' would mean that the all ions were distinguishable and bright, i.e. the image was clear, such as Fig. 2.1a and Fig. 2.1b.

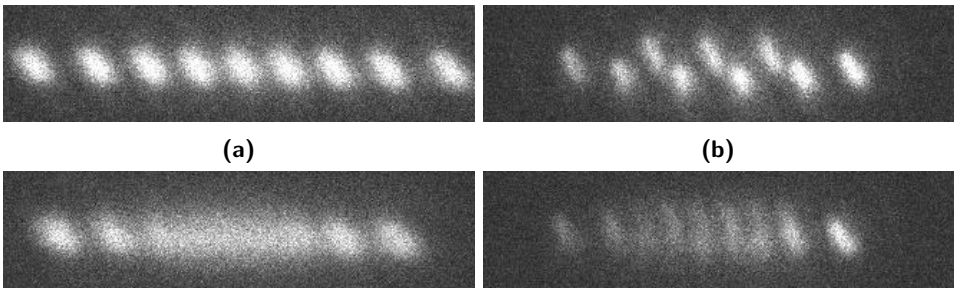

Figure 2.1: Example of possible ion configurations. (a) Nine distinguishable ions in a straight line. (b) Nine distinguishable ions in a zigzag configurations. (c) Nine partially indistinguishable ions in a straight line. (d) Nine partially indistinguishable ions in a zigzag configuration.

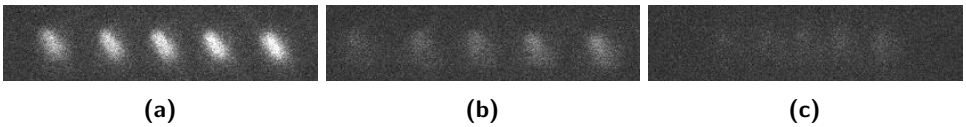

Figure 2.2: Examples for the brightness scale used in the boundary analysis. (a) Five bright ions. (b) Five dim ions. (c) Five very dim ions.

The goal was to identify the set of endcap voltage pairs (V_{left}, V_{right}) which produce a clear image, plot these pairs in the parameter space and find boundary functions $V_{\text{right}}^{\text{max/min}} = f_{\text{boundary}}(V_{\text{left}})$ above/below which (V_{left}, V_{right}) would no longer produce clear images. We didn't consider the entire parameter space $V_{\text{left / right}}$, as we knew that the endcap voltages would need to be nearly symmetrical for the trap not to lose ions. A large asymmetry would shift the minimum of the potential too far from the center of the trap, in which case

[1] A *clear* image of ions will be defined as an image where each ion can be distinguished from its neighbor, and all ions are bright enough to be identified by the human eye.

the ions would no longer be in the focus of the Doppler cooling laser, and hence gain enough kinetic energy to escape the trap. A transformation into the *axial* coordinates, $V_{\text{compression}}$ and V_{shift}, helps us describe that effect. The coordinates are defined as

$$V_{\text{compression}} = 0.5(\frac{V_{\text{left}}}{r} + V_{\text{right}}) \tag{2.1}$$

$$V_{\text{shift}} = 0.5(V_{\text{right}} - \frac{V_{\text{left}}}{r}), \tag{2.2}$$

where $V_{\text{left}}/V_{\text{right}}$ is the voltage applied to the left/right endcap with respect to the video image, and r is an experimental ratio used to compensate for an effective unintentional asymmetry between the true endcap voltages. Eq. 2.2 can be rearranged to give

$$V_{\text{left}} = r(V_{\text{compression}} - V_{\text{shift}}) \tag{2.3}$$

$$V_{\text{right}} = V_{\text{compression}} + V_{\text{shift}}. \tag{2.4}$$

These equations show that when $V_{\text{shift}} = 0$ and a change in $V_{\text{compression}}$ occurs, the ions should simply be pushed closer together without changing their median position, as the minimum of the harmonic potential would still lie in the center of the trap. Here, the *median* position of the ions is the median of the coordinates of all ions in the trap. A change in V_{shift} should shift the minimum of the harmonic potential, and hence change median position of the ions. We would expect that the ions would be off screen or too dim if V_{shift} differs strongly from zero, that the ions would become indistinguishable if $V_{\text{compression}}$ becomes too large, and we know that $V_{\text{compression}}$ must be positive to produce a positive trap frequency. We can therefore make an educated guess of the region containing the boundary functions, and restrict the scan to only this region, instead of scanning the entire parameter space.

The setup was known to display some asymmetry before the start of this project, and we attempted to compensate it by estimating the position of the center of the trap, and optimizing the value of r until the axial coordinates displayed the described behaviour. The value of r found was $r = 1.4$, which is used in the rest of this section.

The boundary analysis depends on the number of ions in the trap, n. The minimum of the potential energy, around which the ions are centered, does not depend on the number of ions, but the Coulomb repulsion term does, so the distance between the ions will depend on the number of ions. Specifically, the more ions are in the trap, the closer the distance between the ions at the same endcap voltages. It is therefore possible that all the ions are distinctly visible at a certain set of endcap voltages, but when n is increased the ions will be indistinguishable. It is also possible that increasing n will simply cause some of the ions to be outside of the frame. The analysis of the boundary voltages was therefore done separately for each n, where $n \in \mathbb{N}$, $1 \leq n \leq 15$.

For each n the Python script scanned through several hundred combinations of the endcap voltages, saving the images of the ions. We then viewed all saved images and made a qualitative estimate of their brightness according to Fig. 2.2, as well as deciding if the ions were distinguishable and within frame. This data analysis was not fully automatic, as the image analysis script by Albert produces unreliable results when all the ions are dim, not clearly distinguishable or in a zigzag configuration. Fig. 2.3 shows some of the results, where the quality category 'zero' is shown in red, 'one' is shown in orange, 'two' is shown in light green and 'three' is shown in dark green on Fig. 2.3.

None of the measured data points lead to a loss of ions from the trap. This includes all data points in which the ions were not visible or indistinguishable on the video stream. It should be noted that the laser intensity strongly influences the brightness of the ions. The lasers on the setup can be periodically unstable, in which case the ions may not be clearly visible even when voltages fulfill the boundary function conditions. The data in this section was only taken when the laser frequencies were locked, and when the intensities were above 60 %. Some fluctuations in the laser intensities were unavoidable, so the brightness scale was still relative to the current intensity of the laser, which is why it is not possible to quantitatively describe the brightness scale described above.

Fig. 2.3 shows that it is possible to describe the set of parameters leading to a clear image with four linear boundary functions, $V_{\text{shift}}^{\text{max/min}} = V_{\text{compression}}\ p_1 + p_0$, two of which describe an upper limit on V_{shift}, and the other two of which describe a lower limit on V_{shift}, each depending on $V_{\text{compression}}$. These boundary functions were fitted to the data by hand. A table with all the parameters is shown in Appendix B, and Fig. 2.3 shows the boundary functions for six and fifteen ions.

We can conclude that large values of $|V_{\text{shift}}|$ will lead to a poor image quality. The maximum possible $|V_{\text{shift}}|$ that leads to a clear image depends on $V_{\text{compression}}$. There is also evidence that a large $V_{\text{compression}}$ leads to a poor image quality, which was due to the ions becoming indistinguishable. We can also conclude that the assumption, that the number of ions would influence the results, was correct, as the boundary functions clearly depend on the number of ions in the trap. It is therefore always necessary to determine the number of ions in the trap before changing the endcap voltages.

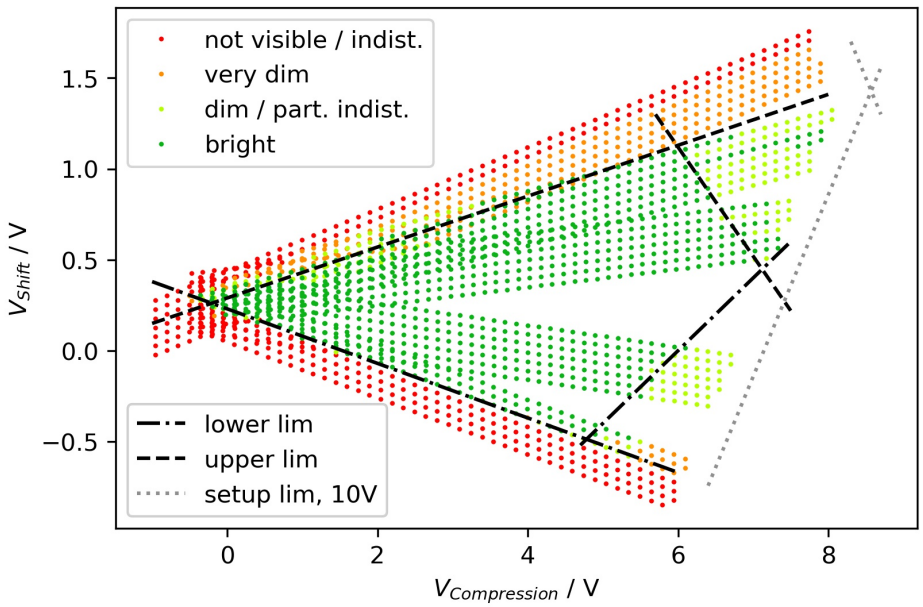

(a)

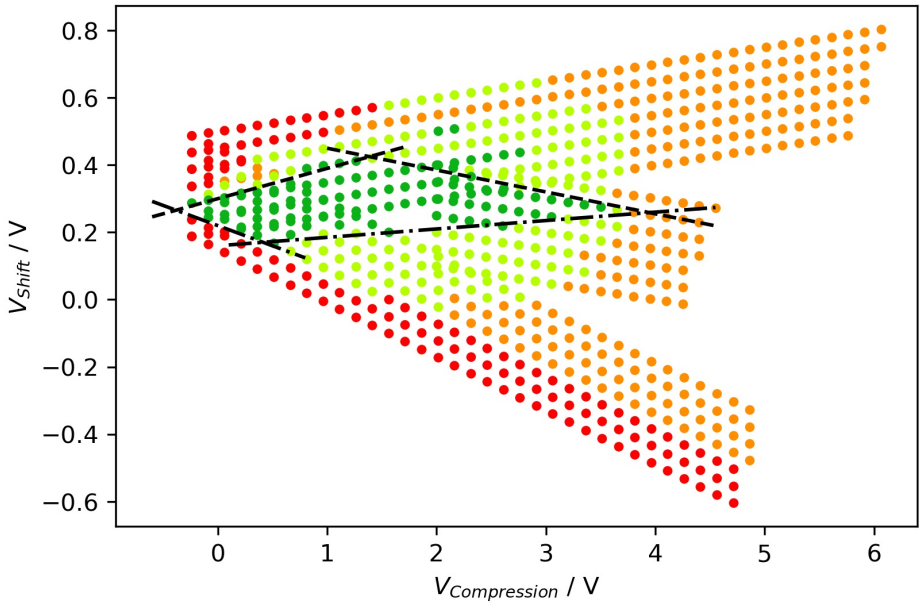

(b)

Figure 2.3: Examples of the boundaries found for (a) six ions and (b) fifteen ions. The black lines show the chosen linear boundaries functions for the voltages that should be applied. The grey lines show the physical limitations of the endcaps, which could not be supplied with more than 10 V.

2.3 Asymmetries in the endcap voltages

2.3.1 Partial compensation of the asymmetry

Initially, we attempted to compensate for the setups inherent asymmetry with the axial coordinates (Eq. 2.2) using $r = 1.4$, as it displays a strong linearity between V_{shift} and the position of each ion when $V_{\text{compression}} = 1$ (Fig. 2.4). The Pearson correlation coefficient was smaller than -0.99 for all ions. However, the median position of the ions is not constant when varying $V_{\text{compression}}$ while $V_{\text{shift}} = 0$ (Fig. 2.5a). We conclude that $r = 1.4$ does not compensate the asymmetry fully.

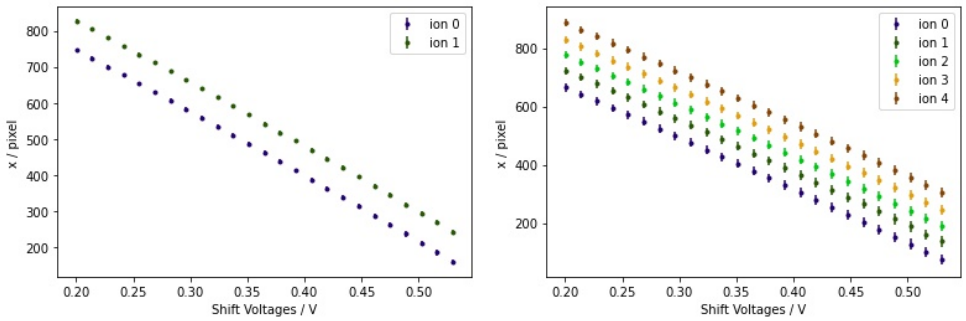

(a) **(b)**

Figure 2.4: Relationship of the position of the ion to the shift voltage, V_{shift}, while $r = 1.4$ and $V_{\text{compression}} = 1$, for (a) two trapped ions and (b) five trapped ions. Each data point was taken two times during different scans and averaged.

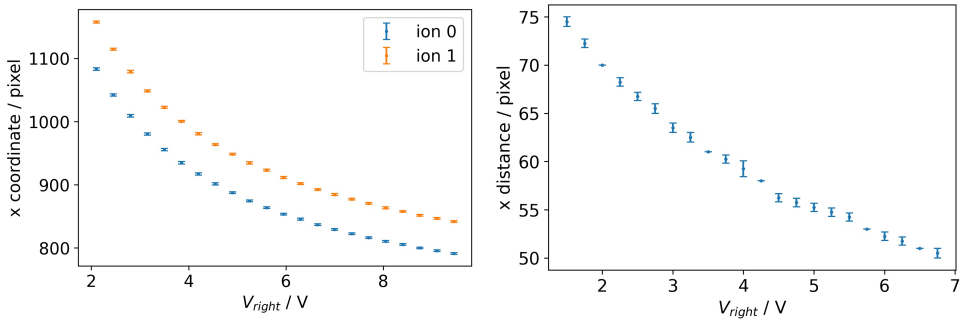

(a) **(b)**

Figure 2.5: Relationship of the (a) position of the ion and (b) distance between the ions to the compression voltage, while $r = 1.4$ and $V_{\text{shift}} = 0$. Each data point was taken four times during different scans and averaged. All data is taken with 2 ions in the trap.

2.3.2 Analysis of the asymmetry

To analyse this asymmetry systematically, a scan of around 500 combinations of left and right endcap voltages within the previously defined boundaries was performed, and the coordinates of the ions were recorded. The average position and average distance between the ions depending on the voltages is shown in Figure 2.6.

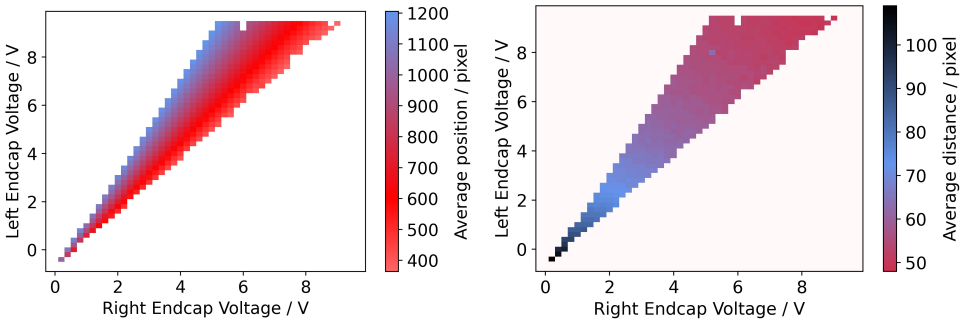

Figure 2.6: Heatplots of (a) the average position of two ions and (b) the average distance between 2 ions when varying the endcap voltages independently. The 1st pixel is the left most pixel on the image, and the center of the trap is estimated to be between between the 750th and 1000th pixel. Note that we are able to apply negative voltages to the left endcap without losing the ions from the trap, which should not be possible.

We can observe an asymmetry in the trap, as the left endcap voltage must be set higher than the right one for stable centered trapping. We suspect that this might be due to coupling between the radio frequency line and the static line connected to the left endcap. There is evidence for a linear relationship between the effective right and left endcap voltage, so the axial coordinates (Eq. 2.4) could potentially be used to compensate for the asymmetry if an appropriate value of r and an additional offset value k added to the left endcap voltage was chosen. While Fig. 2.6a can be used to find a range of plausible r and k values ($1.3 \leq r \leq 1.5, -0.2 \leq k \leq 0.8$), it cannot help with an accurate determination of r and k as the location of the center of the trap is not known.

2.3.3 Finding symmetric endcap voltages

Eq. 1.1 only holds for a symmetric potential, and therefore cannot be applied when the endcap voltages are not symmetric. The main feature of symmetric pairs of voltages would be that they should all leave the median position of the ions unchanged and at the center of the trap. Since the location of the center of the trap is not accurately known, an estimate had to be made. Figure

2.7 shows three dashed/dotted lines with a linear relationship between the voltage of the right and left electrode, which follow the contour lines of the heatmap, which shows the mean position of the ions. The three lines are therefore candidates of such symmetric voltages, as the median position of the ions is near the estimated center of the trap, and does not change along the lines. The first line slightly underestimates the center of the trap, the second should be a good estimate and the third slightly overestimates the center of the trap. These three lines give us information about the effect that a bad estimation of the trap center could have in Sec. 3.2.

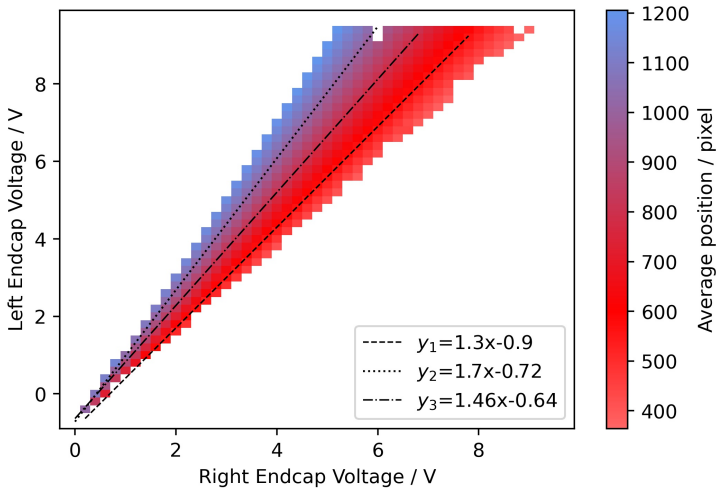

Figure 2.7: Heatplot of the average position of two ions when varying the endcap voltages independently. The first pixel is the left most pixel on the image, and the center of the trap is estimated to be between between the 600th and 900th pixel. The dashed/dotted lines show three candidates for symmetric voltages. The contour heights of y_1, y_2 and y_3 are 528 ± 10, 696 ± 10 and 864 ± 10 respectively.

Chapter 3

Design of an elementary charge experiment

Ideally, the Paul trap at SSCT should not only allow visitors to see the Barium ions with their own eyes, but is should also convey some of the underlying properties of these ions. For this purpose, SSCT offers workshops for student classes, which allow students to carry out experiments that let them explore certain scientific concepts in more detail.

A candidate for such a workshop would be an experiment designed to find the value of the elementary charge e, which would be equal to the charge of the trapped Ba^+ ions. The students should be familiar with the concept of a charge, and may have even determined the elementary charge with Millikan's oil drop experiment [15]. While Millikan's experiment does lead students to think about the role of mass and charge in fundamental forces such as gravity and electrostatic forces, the execution of the experiment is not very inspiring, and it does not provide a good insight into the methods and equipment used in modern science. The theory used in Millikan's experiment may be more accessible to students than the derivation of Eq. 1.2, but it is not the goal of SSCT to convey the theory in detail, and it could be reduced to only the necessary equations. Instead, the goal is to allow the students to explore a physical concept in a more intuitive way, and generate some fascination for science in the process. Since students would be able to see the behaviour of the single charges with their own eyes, and would get insights into measuring techniques and equipment used in more modern experiments, we believe that this experiment could be suitable for a workshop at SSCT.

The experiment could be done by measuring the minimal distance between ions in the trap, and using Eq. 1.2, which can be rearranged to find e. It could realistically be carried out by high school students, as they would only need to measure the distance, in pixels, between the ions on the video stream, which could be done by providing them with axes showing the pixel

number on the image, and letting them estimate the distance with a method of their choosing, for example with a ruler. The students would then require a formula for the trap frequency, which will be derived in Sec. 3.1, a formula for the conversion of pixels to SI units (Eq. 1.3), and the equation for the minimal distance between trapped ions (Eq. 1.2), which can be provided on the instruction sheet.

The goal of this part of the semester project was to determine the trap frequency depending on the endcap voltages, carry out the experiment, and determine whether it can be used to find accurate values for the elementary charge e.

3.1 Trap frequencies

The trap frequency ν from Eq. 1.1 can be found with the help of a simulation of the experimental setup in COMSOL Multiphysics®. The software was given the voltages on the electrodes as boundary conditions, and then generated the electric potential by solving Poisson's equation [16]. Since the electric potential along the symmetry axis is harmonic (Eq. 1.1), it was fitted to a quadratic of the form $V = a_2 z^2 + a_0$, where $z = 0$ is the center of the trap, and a_0 is the arbitrary offset of an electric potential. The fit was done for a range of different endcap voltages from 0.25 V to 9.75 V. The assumption in this simulation was that the radio frequency electrodes would not affect the trap frequency on this axis, and would therefore not have to be simulated. Examples of the fit are shown in Fig. 3.1.

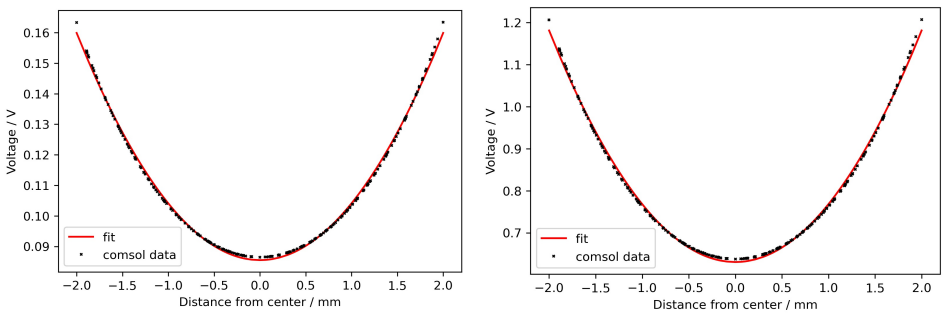

Figure 3.1: Electric potential of the trap along the symmetry axis for different endcap voltages, simulated with COMSOL Multiphysics®. The data was fit to a quadratic, $V = a_2 z^2 + a_0$.

The quadratic coefficients were then plotted against their respective endcap voltages (Fig. 3.2), and fit to a linear function, which was

$$a_2 = 0.0149\ \text{mm}^{-2} * V_{\text{endcap}} - 2.14 \times 10^{-6}\ \text{V mm}^{-2}, \tag{3.1}$$

where V_{endcap} are the endcap voltages V_{right} and V_{left}. Students could now carry out the elementary charge experiment for arbitrary symmetric voltages $0 < V_{\text{endcap}} < 10$, as we can use this equation to find the trap frequency for any V_{endcap} in this range.

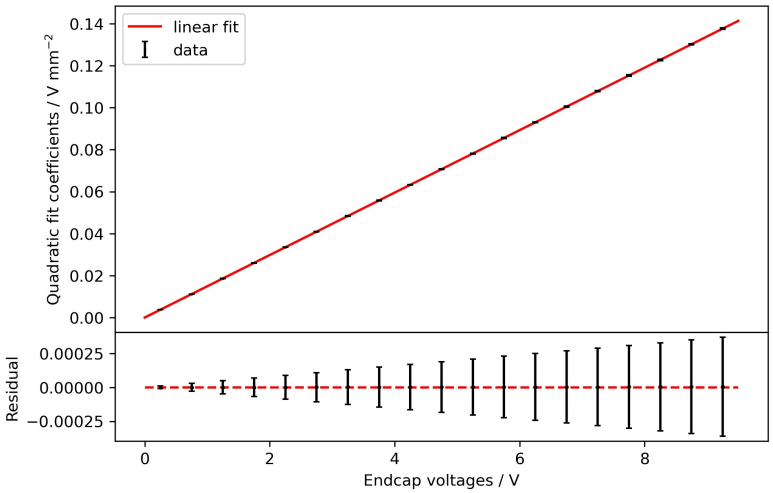

Figure 3.2: Relationship between the voltage applied to both endcaps and the quadratic fit coefficient a_2 from Fig. 3.1. The uncertainties are derived from the covariance matrices of the quadratic fits. The data was fit to a linear function, shown in red. The residuals plot shows that the linearity is very strong, which is supported by the Pearson product-moment correlation coefficient [17] of $r = 1.0$.

For a charge in an electrostatic field, the electric potential V_{el} and the energy of the charge V_{energy} obey the relation $V_{\text{el}} * C = V_{\text{energy}}$, where C is the charge of the object. Hence we can compare the quadratic coefficients of the simulation and the theoretical formula for the trap potential (Eq. 1.1) to find

$$\nu^2 = \frac{2\, a_2\, Z\, e}{M}, \tag{3.2}$$

where ν is the trap frequency, a_2 the fit coefficient (Fig. 3.1), Z the charge number of the ion, e the elementary charge and M the mass of the trapped ion.

Using Eq. 1.2 and Eq. 3.2 we can then find expressions for the charge of the ions depending on experimental parameters,

$$\begin{aligned} N = 2: &\ Z\, e = 4\, \pi\, \varepsilon_0\, a_2\, \Delta z_{\text{min}}^3 \\ N = 3: &\ Z\, e = 6.4\, \pi\, \varepsilon_0\, a_2\, \Delta z_{\text{min}}^3 \\ N = n: &\ Z\, e \approx 8\pi\, \varepsilon_0\, a_2 (\frac{\Delta z_{\text{min}}\, n}{2.018})^3, \end{aligned} \tag{3.3}$$

which can be given to the students instead of Eq. 1.2.

3.2 Measurement of the elementary charge

The measurements of the electron charge according to the candidates for symmetric voltages from Sec. 2.3.3 were repeated four times each, and are shown in Fig. 3.3. It is clear that nearly all the data points differ from the literature value, $e = 1.602176634 \times 10^{-19}$ C [18], by a factor larger than ten. Fig. 3.3 shows that the measurement electron charges increased when the endcap voltage was increased, which means that the main source of error is dependent on the voltage applied.

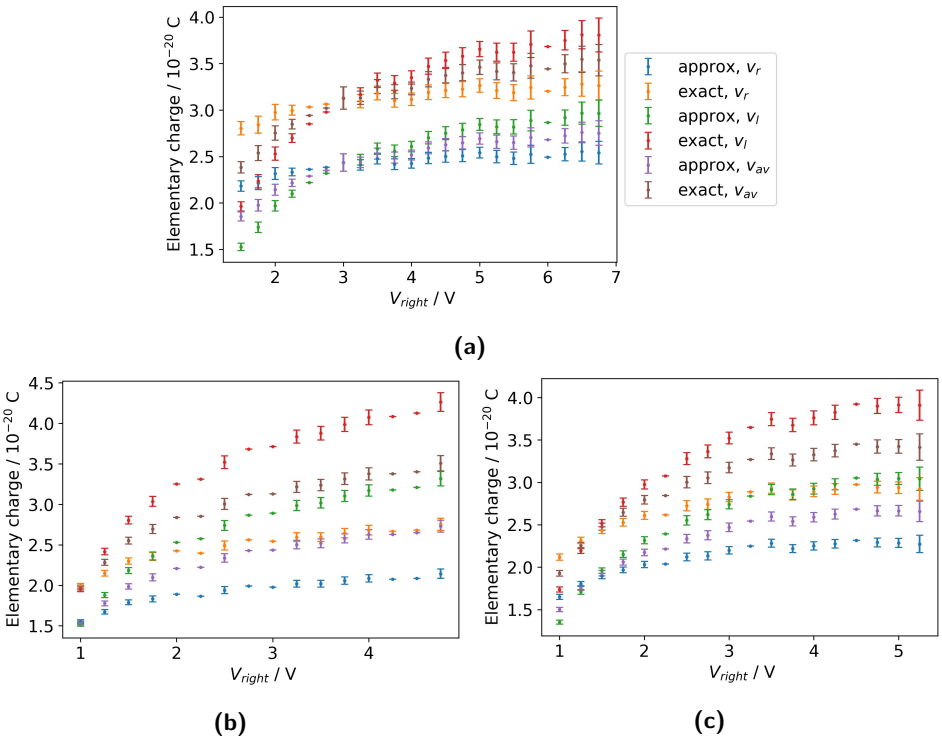

Figure 3.3: Relationship between the measured electron charge depending on the voltages set on the electrodes. The voltage of the left endcap was (a) $V_{\text{left}} = 1.3V_{\text{right}} - 0.9$ V, (b) $V_{\text{left}} = 1.7V_{\text{right}} - 0.72$ V and (c) $V_{\text{left}} = 1.46V_{\text{right}} - 0.64$ V. All measurements were done with two ions. The coefficient a_2 was determined according to the linear fit in Figure 3.1, and was calculated once with respect to the right endcap voltage (labelled v_r), once with respect the the left endcap voltage (labelled v_l) and once with their mean (labelled v_{av}). Each charge was calculated with the exact formula for two ions and the approximation for n ions shown in equation 3.3. Each data point was taken four times in different measurement runs, and the errorbars show their standard deviation.

A possible error source for this experiment is that we did not accurately supply the trap with a symmetric potential around the center of the trap, so theory may not correspond to the experiment. Fig. 2.7 provides three estimates for symmetric voltages, for which y_1 likely underestimates the

position of the center of the trap, and y_2 likely overestimates the position of the center of the trap, and yet all three candidates gave similarly bad estimates for the value of the elementary charge, so it is unlikely that this is the main error source.

It is also possible that the voltages that reach the electrodes differ from the applied voltages on both sides, which would mean that we were using a trap frequency corresponding to the wrong endcap voltages in the calculations. According to Eq. 3.3 the calculated charge varies linearly with the trap frequency, and Fig. 3.2 shows that the voltage at the endcap would have to be more than three times larger than the voltage set by the DAC to explain the discrepancy of the measured results. This is very unlikely.

Another source of errors could be the estimation of the trap frequency. The assumption, that the radio frequency field does not affect the trap frequency along the symmetry axis, may not hold true, which would affect all final results. This assumption could be tested by simulating the full trap including the radio frequency field in MATLAB®.

Chapter 4

Discussion

4.1 Discussion of ion positions

In Sec. 2.2 we successfully found boundary values for the voltages of the endcap electrodes that produce a clear image of the trapped ions. This has allowed us to implement a function that determines if the requested voltages are safe[1], which simplifies the daily operation of the setup. For example, this function will be useful in any future data analysis, as we can now avoid the loss of electrons in further experiments. It would also allow us to provide visitors with another interactive feature of the setup, in which they could move the ions around the symmetry axis without supervision. This could be done by providing them with a button or sliding scale, where they can change the voltage of the left and right endcap independently, and then observe what happens. A question sheet could be provided, which would ask the visitors simple questions, such as: 'What is the sign of the charge of the Barium ion?', or 'How can we move the ions into a zigzag configuration?'. This could make the exhibit more interactive for all age groups.

In Sec. 2.3 we characterized asymmetries inherent to the setup, and discussed how these asymmetries might be compensated using an appropriate transformation of the voltages (Eq. 2.2). However, we were only able to make estimations for such a transformation, as we did not locate the center of the trap precisely. While the asymmetries in the setup do not influence the daily operation, they will be important in all workshop experiments that rely on an accurate knowledge of the electric field within the trap. It would therefore be important to accurately determine the location of the trap center for potential future projects.

[1] Here, a *safe* voltage should be understood as a voltage that will provide a clear image of the ions, and hence cannot disturb the exhibit.

4.2 Discussion of the elementary charge experiment

Sec. 3.1 provides us with an equation of the trap frequencies, which is an important part of characterizing our Paul trap, as they provide us with a quantitative formula for the electric potential along the symmetry axis when used in combination with Eq. 1.1. These trap frequencies have not been experimentally tested, which could be done by applying a voltage to the endcaps that oscillates at the respective theoretical trap frequency. If these frequencies correspond to the true trap frequencies, the ions should be in resonance with this alternating field and would visibly oscillate along the symmetry axis.

Since the equation for the harmonic trap potential, Eq. 1.1, is an approximation that only holds in the center of the trap, it is possible that the range of z values used for the quadratic fit in Fig. 3.2 was too large, leading to an overestimation of the trap frequencies. A more suitable range of z values would have been between -100 µm and 100 µm, as the ions are contained within this region. It is therefore possible that, when testing the trap frequency using the alternating voltages, the oscillation of the ions would be observed at a lower frequency than predicted.

If an oscillation cannot be observed at all, it may be due to an incorrect assumption that the radio frequency electrodes do not affect the electric field on the symmetry axis. In this case we should simulate the full trap in MATLAB®. This would also give us the necessary information to find the radial trap frequency, and hence fully characterize the electric field within the trap.

The measurement of the elementary charge in Sec. 3.2 did not give accurate results. The proposed experiment for the SSCT workshop is therefore not ready to be offered to students. Overcoming the limitations caused by the asymmetry of the endcap electrodes and testing the theoretical trap frequencies would likely require significantly more analysis of the setup, so it may be easier to design a workshop experiment based on the lifetime of the dark state in the mean time instead.

Appendix A

Derivation for the smallest distance between trapped ions

Eq. 1.1 can be used to find the minimum distance between n trapped ions numerically. In the case of 2 or 3 ions, this solution can also be found analytically. This derivation is based on the derivation laid out in [6].

Let us assume that our system has been cooled down enough to be able to neglect thermal motion to first order. In that case the minimal energy solution to Eq. 1.1 will be stationary, $z_m(t) \approx z_m$, and can be found with the ansatz

$$\begin{aligned}\frac{\partial V}{\partial z_m} &= \sum_{m=1}^{N} M\nu^2 z_m \\ &+ \sum_{n=1}^{m-1} \frac{Z^2e^2}{8\pi\varepsilon_0} \frac{z_n - z_m}{|z_n - z_m|^3} + \sum_{n=m+1}^{N} \frac{Z^2e^2}{8\pi\varepsilon_0} \frac{z_n - z_m}{|z_n - z_m|^3} \\ &+ \sum_{n=1}^{m-1} \frac{Z^2e^2}{8\pi\varepsilon_0} \frac{z_n - z_m}{|z_m - z_n|^3} + \sum_{n=m+1}^{N} \frac{Z^2e^2}{8\pi\varepsilon_0} \frac{z_n - z_m}{|z_m - z_n|^3} \\ &= 0.\end{aligned}$$

Using the substitution $u_m * l = z_m$, where $l^3 = \frac{Z^2e^2}{4\pi\varepsilon_0 M\nu^2}$, we can simplify this to

$$\sum_{m=1}^{N} u_m + \sum_{n=1}^{m-1} \frac{u_n - u_m}{|u_n - u_m|^3} + \sum_{n=m+1}^{N} \frac{u_n - u_m}{|u_n - u_m|^3} = 0. \tag{A.1}$$

For $N = 2$ this is

$$u_1 + \frac{u_2 - u_1}{|u_2 - u_1|^3} = 0,$$
$$u_2 + \frac{u_1 - u_2}{|u_1 - u_2|^3} = 0,$$

which simplifies further if we assume $u_2 > u_1$,

$$u_1 + \frac{1}{(u_2 - u_1)^2} = 0,$$
$$u_2 - \frac{1}{(u_1 - u_2)^2} = 0.$$

Now we can see that $u_1 = -u_2$, which can be substituted to find

$$u_1 = -\left(\frac{1}{4}\right)^{1/3}, \quad u_2 = \left(\frac{1}{4}\right)^{1/3}, \tag{A.2}$$

as suggested by Eq. 1.2.

Appendix B

Parameters of the boundary functions of the endcap voltages

The parameters of the boundary functions from section 3.1 can be found in Table 1.

Boundary Coefficients								
N_{ions}	$p_0^{\text{t, l}}$	$p_0^{\text{t, r}}$	$p_0^{\text{b, l}}$	$p_1^{\text{b, r}}$	$p_1^{\text{t, l}}$	$p_1^{\text{t, r}}$	$p_1^{\text{b, l}}$	$p_1^{\text{b, r}}$
1								
1	0.31	9.5	0.27	-6.79	0.122	-1	-0.184	1
2	0.27	9.5	0.23	-6.79	0.112	-1	-0.17	1
3	0.31	9.5	0.27	-6.79	0.116	-1	-0.183	1
4	0.31	9.5	0.25	-6.79	0.1	-1	-0.162	1
5	0.31	9.5	0.23	-6.79	0.125	-1	-0.15	1
6	0.29	4.72	0.23	-2.4	0.14	-0.6	-0.15	0.4
7	0.31	5.5	0.25	-2.5	0.07	-1	-0.162	0.6
8	0.31	0.85	0.25	-1.28	0.097	-0.15	-0.162	0.26
9	0.32	13.3	0.22	-0.16	0.1	-1.8	-0.16	0.06
10	0.35	3.73	0.31	-0.06	0.05	-0.5	-0.16	0.06
11	0.28	1	0.165	-0.15	0.08	-0.05	-0.12	0.11
12	0.3	1.03	0.22	-0.12	0.09	-0.1	-0.12	0.125
13	0.3	1.03	0.23	0.1	0.08	-0.15	-0.14	0.045
14	0.3	0.35	0.22	0.01	0.09	0.04	-0.12	0.14
15	0.3	0.515	0.22	0.16	0.09	-0.065	-0.12	0.025

Table B.1: Table showing the parameters of the boundary functions found in section 3.1. The superscript t/b stands for a upper/lower boundary function, and the superscript r/l stands for a right/left boundary function, analogously to Fig. 2.3.

Bibliography

[1] Manuel Vogel. *Particle Confinement in Penning Traps*, volume 100. Springer International Publishing AG, Gewerbestrasse 11, 6330 Cham, Switzerland, 2018.

[2] J.R. Pierce. *Theory and Design of Electron Beams*. Springer International Publishing AG, 1949.

[3] Nicolai Friis, Oliver Marty, Christine Maier, Cornelius Hempel, Milan Holzäpfel, Petar Jurcevic, Martin B. Plenio, Marcus Huber, Christian Roos, Rainer Blatt, and Ben Lanyon. Observation of Entangled States of a Fully Controlled 20-Qubit System. *Phys. Rev. X*, 8:021012, Apr 2018.

[4] Swiss Science Center Technorama. Swiss Science Center Technorama, 2022. [Online; www.technorama.ch; accessed June 28, 2022].

[5] S. Earnshaw. On the Nature of the Molecular Forces which regulate the Constitution of the Luminiferous Ether. *Trans. Camb. Philos. Soc.*, 7:97, 1842.

[6] D.F.V. James. Quantum dynamics of cold trapped ions with application to quantum computation. *Applied Physics B*, 66:181–190, 1998.

[7] Todd P. Meyrath and Daniel F. V. James. Theoretical and Numerical studies of the positions of cold trapped ions. *Physics Letters A*, 240:37–42, 1998.

[8] A. Steane. The ion trap quantum information processor. *Applied Physics B*, 64:623–642, 1997.

[9] Y. Castin, H. Wallis, and J. Dalibard. Limit of doppler cooling. *J. Opt. Soc. Am. B*, 6(11):2046–2057, Nov 1989.

[10] OpenStax. University Physics III - Optics and Modern Physics, February 2022. [Online; phys.libretexts.org; accessed June 28, 2022].

[11] Michael DePalatis. Barium Energy level diagrams. [Online; mike.depalatis.net; accessed June 28, 2022].

[12] Douglas S. Goodman. Magnification equations for a two-lens system. *Appl. Opt.*, 24(12):1732–1732, Jun 1985.

[13] CMOS Camera Expert. ASI290MM (mono). [Online; astronomy-imaging-camera.com; accessed June 28, 2022].

[14] Albert Mitjans-Coma. Ion trap image analysis. Semester Project, Trapped Ion Quantum Information Group, ETH Zurich, June 2021.

[15] Marco Di Mauro. The millikan oil drop experiment. In *Modern Physics*, 2053-2563, pages 14–1 to 14–17. IOP Publishing, 2020.

[16] Masud Chaichian, Ioan Merches, Daniel Radu, and Anca Tureanu. *Electrodynamics*. Springer Berlin, Heidelberg, 2016.

[17] Jennifer Chee. Pearson's product-moment correlation: Sample analysis. 01 2013.

[18] CODATA Task Group on Fundamental Constants. The NIST Reference on Constants, Units, and Uncertainty, 2018. [Online; https://physics.nist.gov; accessed July 1, 2022].

ETH

Eidgenössische Technische Hochschule Zürich
Swiss Federal Institute of Technology Zurich

Declaration of originality

The signed declaration of originality is a component of every semester paper, Bachelor's thesis, Master's thesis and any other degree paper undertaken during the course of studies, including the respective electronic versions.

Lecturers may also require a declaration of originality for other written papers compiled for their courses.

I hereby confirm that I am the sole author of the written work here enclosed and that I have compiled it in my own words. Parts excepted are corrections of form and content by the supervisor.

Title of work (in block letters):

ION RESPONSE TO ENDCAP VOLTAGE VARIATIONS IN A LINEAR PAUL TRAP

Authored by (in block letters):

For papers written by groups the names of all authors are required.

Name(s):	**First name(s):**
BROCKMEYER	FREDERIKE

With my signature I confirm that

- I have committed none of the forms of plagiarism described in the 'Citation etiquette' information sheet.
- I have documented all methods, data and processes truthfully.
- I have not manipulated any data.
- I have mentioned all persons who were significant facilitators of the work.

I am aware that the work may be screened electronically for plagiarism.

Place, date	**Signature(s)**
Zürich, 27.07.22	

For papers written by groups the names of all authors are required. Their signatures collectively guarantee the entire content of the written paper.